Capacitively Coupled Electrode Array Sensors for Body Posture and ECG Measurement During Sleep

Article *in* IEEE Access · February 2021

DOI: 10.1109/ACCESS.2021.3057256

IEEE Access
Multidisciplinary : Rapid Review : Open Access Journal

Received January 4, 2021, accepted January 21, 2021, date of publication February 4, 2021, date of current version February 11, 2021.

Digital Object Identifier 10.1109/ACCESS.2021.3057256

Capacitively Coupled Electrode Array Sensors for Body Posture and ECG Measurement During Sleep

SOUSUKE NAKAMURA[1], (Member, IEEE), NAOKI KAMIYAMA[2], (Member, IEEE), YUTO ARIMA[2], AND TETSUO NAKAMURA[3], (Member, IEEE)

[1]Faculty of Science and Engineering, Hosei University, Koganei 184-8584, Japan
[2]Graduate School of Science and Engineering, Hosei University, Koganei 184-8584, Japan
[3]School of Information Science, Meisei University, Hino 191-8506, Japan

Corresponding author: Sousuke Nakamura (snakamura@hosei.ac.jp)

ABSTRACT Holter electrocardiographs, which are commonly used for long-term electrocardiographic measurements, are not necessarily suitable for long-term measurements during sleep because the electrodes are directly attached to the skin, causing discomfort and constraint feelings. To handle this problem, electrocardiogram measurement using capacitively coupled electrodes, which do not require direct skin contact, could be an alternative. However, this method requires precise positioning of the electrodes on specific parts of the body, which makes it difficult to work robustly in response to physical body differences and postural variations such as turning over. Therefore, the authors have been working on the realization of a novel electrocardiogram measurement system using capacitively coupled electrodes arranged in an array. The major feature of this system is the ability to measure both body posture and electrocardiogram with common electrodes arranged in an array, and by selecting the most effective electrodes based on the measured posture, it can make electrocardiogram measurements corresponding to the posture changes. In this paper, as the core of the system, a new sensor that can measure both body posture and electrocardiogram with common arrayed electrodes has been designed and implemented. From the experimental results, it was confirmed that the subject's posture on the electrode array could be obtained from the distribution of capacitance, and also the electrocardiogram of the subject could be obtained with the same electrodes as well.

INDEX TERMS ECG measurement, body posture measurement, capacitively coupled electrode array, bed sensor.

I. INTRODUCTION

There are high expectations for preventive medicine, such as health management and detection of signs of disease by collecting large amounts of biometric information on a daily basis over a long period of time. For example, long-term electrocardiographic measurements have been shown to be useful in the detection of heart disease, one of the three major causes of death in Japan, with a mortality rate of about 15% [1]. To detect transient arrhythmias and ischemic heart disease (e.g., angina pectoris, myocardial infarction, etc.), long-term recording is required, so electrocardiograph for 24-hour measurement such as Holter electrocardiographs have been used in medical institutions. However, the fact that electrodes need to be directly attached to the skin, causing discomfort and constraint feelings, makes it unsuitable for long-term measurements during sleep.

To handle this problem, one potential alternative is to use capacitively coupled electrocardiographic electrodes that do not need to be directly attached to the skin [2], [3]. In this measurement method, the electrodes connected to the measurement circuit are capacitively coupled to the surface of the human body through clothing to form a capacitor, which provides an electrical connection between the human body and the measurement circuitry [4]. Therefore, by placing electrodes on the bed, electrocardiographic measurements can be made without wearing any device, enabling measurements by simply having the subject lie down.

However, while the device is comfortable, it is necessary to place each electrode (e.g., selecting three electrodes such as

The associate editor coordinating the review of this manuscript and approving it for publication was Mohammad Zia Ur Rahman.

+, −, GND for three-point leads) close to the appropriate part of the body for stable measurement, which limits the position and posture (hereafter collectively referred to as *posture*) for reliable measurement. This means that special measures are needed to deal with the changes in the human body's posture caused by turning over.

To address these issues, Ueno *et al.* proposed a system that can respond to changes in body posture to a certain extent by utilizing the electrodes designed to be the same size as the width of the bed [5]. However, this configuration requires electrode arrangement according to each person's body physique and is difficult to adapt to changes in vertical movement on the bed, suggesting room for improvement in robustness in terms of responding to body size and postural variations.

Incidentally, for measurement of biometric signal that is robust with respect to body shape and posture during sleep, one of the effective approach is to use arrayed sensors which can both measure body posture and biometric signal. Here, arrayed sensors estimate the body posture during sleep at first, and then the biometric signal is measured with specific sensors selected based on this posture information.

Posture measurement on the bed utilize the distribution of pressure and capacitance measured by sensors laid out in an array configuration, such as pressure measurement based on piezoresistive effect [6] - [9], optical pressure measurement using optical fiber [10], pressure measurement based on piezoelectric effect [11], capacitive pressure sensors sandwiched between dielectrics [12], [13], and capacitance measurement using flat plate electrodes [14]–[17].

Among these examples, there are studies that have converted the array of sensors used for posture measurement to biometric measurements, including those that measured respiratory activity in addition to posture [8], [15], [16], respiratory activity and heart rate in addition to posture [9], [13], ballistocardiogram and heart rate in addition to posture [11], and respiratory activity, heart rate and ballistocardiogram in addition to posture [17].

For example, Mukai *et al.* measured posture from the pressure distribution using an array of pressure sensors and measured respiration and heart rate from the time-series information of specific pressure sensors selected based on postural information [13]. Chang *et al.* measured posture from the distribution of capacitance using an array of capacitance sensors and measured respiration from the time-series information of specific capacitance sensors selected based on the posture information [15].

However, it should be noted that none of them dealt with electrocardiographic measurements because most of these methods are designed to evaluate the quality of sleep, including insomnia and sleep disorders, and therefore, the measured cardiac activity was limited to heart rate or ballistocardiogram.

In these circumstances, the authors have been working on the realization of a novel electrocardiogram measurement system using capacitively coupled electrodes arranged in an array, which work robustly in response to body physical differences and postural variations such as turning over. The major feature of this system is the ability to measure body posture and electrocardiogram with common electrodes arranged in an array, and by selecting the most effective electrodes based on the measured posture, it can measure electrocardiogram regarding the posture changes without searching all combinations of the electrodes.

In this paper, a new sensor that can measure both body posture and electrocardiogram with common arrayed electrodes has been designed and implemented as the core of the system, and its effectiveness has been verified through evaluation experiments.

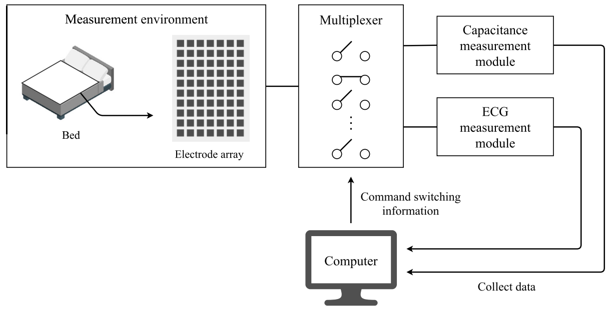

FIGURE 1. The configuration of the proposed sensor. The computer provides commands to the multiplexer for switching between modules, and collects the measured data from them.

II. CAPACITIVELY COUPLED ELECTRODE ARRAY SENSORS FOR MEASURING BOTH BODY POSTURE AND ELECTROCARDIOGRAM

To measure the subject's body posture and electrocardiogram during sleep, we propose the sensor configuration shown in Fig. 1. Also, the actual setup of the sensor is shown in Fig. 2. In the proposed sensor, each of the electrodes arranged in an array can be connected to any of 3 channels (+, −. GND) of the ECG (electrocardiogram) measurement module or 1 channel of the capacitance measurement module by using a multiplexer to arbitrarily switch between these 4 channels. This enables both body posture and electrocardiogram measurements simply by lying on the electrode array placed on a bed.

Firstly, in order to measure the posture, all of the electrodes are connected to the capacitance measurement module one by one by the multiplexer, and the electrostatic capacitance between the human body and each electrode is measured. Then, based on the distribution of capacitance of the electrode array, the silhouette of the subject on the electrodes is acquired, and the posture can be detected.

Next, three electrodes selected in reference to this posture information are connected to the three channels (+, −, GND) of the ECG measurement module by the multiplexer. In this way, the proposed sensor can measure electrocardiograms corresponding to the postural change of the subject.

Here, it should be noted that the measurement of both body posture and electrocardiogram can be made with common

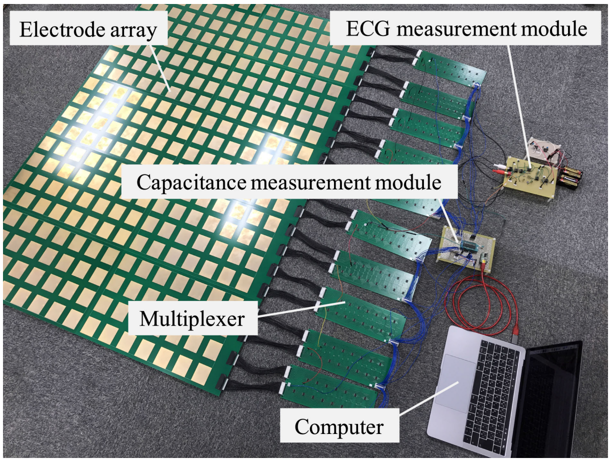

FIGURE 2. The actual sensor setup. The sensor consists of an electrode array, computer, ECG measurement module, capacitance measurement module, and a multiplexer.

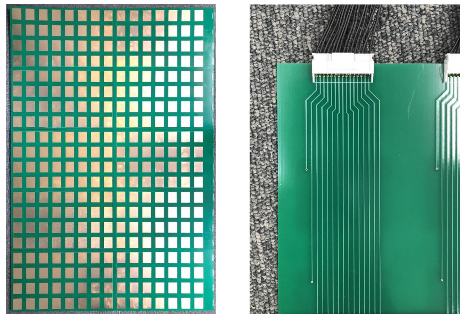

FIGURE 3. The developed electrode array. The electrode array is a double-sided printed circuit board. (a) Electrodes are placed on the surface. The dimension of each electrode is 50 × 40 mm, and they are separated by 20 mm, both vertically and horizontally. The overall size of the electrode array is 1,380 × 880 mm. (b) The wiring is placed on the back side to prevent unnecessary capacitive coupling between the human body and the wiring.

arrayed electrodes because they are both based on the capacitance coupling between the human body and electrodes.

III. DESIGN AND DEVELOPMENT OF CAPACITIVELY COUPLED ELECTRODE ARRAY SENSORS

A. DESIGN AND DEVELOPMENT OF ELECTRODE UNIT

The electrode array which was developed based on a printed circuit board (FR-4) is shown in Fig. 3.

The printed circuit board is double-sided, and electrodes are placed on the surface, while the wiring is placed on the back side to prevent unnecessary capacitive coupling between the human body and the wiring. The electrodes are made of copper, and their surface were treated with an electroless gold plating finish to prevent deterioration. Each electrode was prepared to a size of 50 × 40 mm in length and width taking into consideration the compatibility of posture detection and electrocardiographic performance, after investigating related studies [16], [18]. Specifically, the dimension of the electrode was carefully determined considering the fact that smaller size leads to increased resolution of the capacitance distribution and results in precise posture detection, while it makes the measurement of electrocardiogram difficult due to the reduction of capacitance coupling between the human body. Each electrode is arranged with 20 mm of spacing between them so that they do not interfere with each other. 300 electrodes in 20 rows and 15 columns are arranged to provide a detection range of the electrode array with an overall dimension of 1,380 × 880 mm in length and width.

B. DESIGN AND DEVELOPMENT OF CAPACITANCE MEASUREMENT MODULE

A microcontroller-based constant current source and an AD converter were used as the capacitance measurement module to measure the electrostatic capacity with adjustable measurement range and measurement resolution.

When a current of I [A] flows into a capacitor of capacitance C [F], the voltage V [V] that is charged to the capacitor after the passage of time t [s] can be expressed as;

$$V = \frac{I \cdot t}{C} \tag{1}$$

The basic measurement principle of the capacitance measurement module is to derive the capacitance value C indirectly by measuring the charging voltage V under the specified constant value of current I and charging time t.

Here, the measurement range of the capacitance value is subject to the measurement range of the charging voltage. Moreover, since the capacitance and the voltage are inversely proportional, the capacitance measurement shows variable resolution while the voltage measurement is conducted in a constant resolution through the AD converter. Therefore, since it is obvious that both measurement range and measurement resolution of the capacitance are related to the current I and charge time t, which could be specified by the microcontroller, it could be said that the desired measurement range and measurement resolution could be realized by selecting an appropriate value for I and t.

In the following, the method of selecting these parameter values (constant current I and charging time t) so as to satisfy the given measurement range $C_{min} \leq C_{range} \leq C_{max}$ and the measurement resolution ΔC_{res} of the capacitance, has been introduced.

First, we discuss how to realize the desired measurement range of the capacitance. The measurement range of the voltage that can be measured by the AD converter is expressed as;

$$V_n = \frac{n \cdot V_{ref}}{2^b} \quad (0 \leq n \leq 2^b - 1) \tag{2}$$

while the reference voltage and resolution of the AD converter are expressed as V_{ref} [V] and b [bit], respectively. Then, the minimum and maximum values of the measurable capacitance can be derived by substituting the minimum and maximum values in (2) into (1), and thus the conditions to be satisfied to realize the given measurement range of the capacitance are found to be given by (3) and (4).

$$C_{min} \geq \frac{I \cdot t}{\frac{2^b-1}{2^b} \cdot V_{ref}} \tag{3}$$

$$C_{max} \leq \frac{I \cdot t}{\frac{1}{2^b} \cdot V_{ref}} \tag{4}$$

Next, we discuss how to realize the desired measurement resolution of the capacitance over the given measurement range. The voltage change ΔV when the capacitance changes by ΔC is expressed as;

$$\Delta V = \left| -\frac{I \cdot t}{C^2} \cdot \Delta C \right| \tag{5}$$

by multiplying ΔC to the differentiate (1) with respect to C.

The resolution of the measured voltage of the AD converter, ΔV_{min}, is;

$$\Delta V_{min} = \frac{V_{ref}}{2^b} \tag{6}$$

and the change in voltage below ΔV_{min} could not be detected. Therefore, from (5) and (6), it can be said that (7) must be satisfied to measure the capacitance with the measurement resolution of ΔC in a certain capacitance value C.

$$\left| -\frac{I \cdot t}{C^2} \cdot \Delta C \right| \geq \frac{V_{ref}}{2^b} \tag{7}$$

Finally, the measurement resolution can be guaranteed over the given measurement range by satisfying;

$$\left| -\frac{I \cdot t}{C_{max}^2} \cdot \Delta C_{res} \right| \geq \frac{V_{ref}}{2^b} \tag{8}$$

In conclusion, the desired measurement range (C_{min} and C_{max}) and the measurement resolution (ΔC_{res}) of the capacitance measurement module can be guaranteed by adjusting the parameters (constant current I and charging time t) to satisfy all of (3), (4) and (8).

C. DESIGN AND DEVELOPMENT OF ECG MEASUREMENT MODULE

The block diagram of the signal process in the developed ECG measurement module is shown in Fig. 4. The module was constructed with an instrumentation amplifier, high and low-pass filters, notch filters, and an inversion amplifier, to amplify the signal and remove noise. In addition, the signal lines are shielded and guarded with shielded wires to reduce the inclusion of external noise.

The cutoff frequency of the high-pass filter, low-pass filter and the notch filter were set to 0.5 Hz, 40 Hz, and 50 Hz, respectively. The low-pass filter in the later stage is designed to have a Bessel characteristic in order to suppress the distortion of the electrocardiogram signals due to the phase delay of the filter circuit [19].

The amplification is multiplied by 10 in the instrumentation amplifier and by 10 in the two inverting amplifiers in the latter stage, making the signal 1,000 times larger through the overall circuit.

Moreover, since the performance of common-mode signal rejection is degraded when measurements are made with capacitively coupled electrodes, DRL (Driven Right-Leg) circuits are used to remove common-mode noise that cannot be adequately removed by the instrumentation amplifier alone [20], [21]. In this prototype module, the common-mode signal is extracted from the output of the first stage voltage follower circuit, and inserted into the DRL circuit.

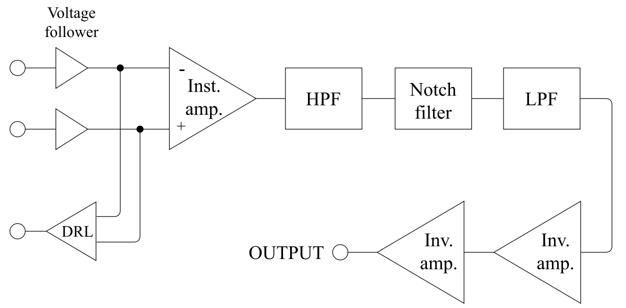

FIGURE 4. Block diagram of the signal process in the developed ECG measurement module.

IV. RESULT

A. EVALUATION OF CAPACITANCE MEASUREMENT PERFORMANCE USING CAPACITANCE MEASUREMENT MODULE

To begin with, the measurement range and measurement resolution of the capacitance measurement module were set up considering the parasitic capacitance values caused by the multiplexer and electrode array wiring, etc., assuming conditions with arrayed configuration. Therefore, since the parasitic capacitance value was about 470 pF in the preliminary measurement in the absence of the object to be measured, the minimum value of the measurement range was set to $C_{min} = 450$ pF with a margin, and the maximum value was set to $C_{max} = 600$ pF, considering the fact that the human body's capacitance value is approximately 150 pF. The measurement resolution was set to $\Delta C_{res} = 1$ pF. The measurement range and measurement resolution of the capacitance measurement module are summarized in Table 1.

Then the performance of the capacitance measurement module was evaluated under the setup shown in Fig. 5, and compared with the measured values of a commercially available LCR meter (LCR-915, Texio Technology). Several capacitors with different capacitance values were prepared as the measurement targets. In order to simulate the actual experimental environment of an electrode array, a capacitor $C_{p2} = 470$ pF representing the parasitic capacitances was connected in parallel with the measurement target C_S. The capacitance value of the measurement target was derived by subtracting the measured capacitance value from the parasitic capacitance value.

TABLE 1. Measurement range and measurement resolution of the capacitance measurement module. C_{min} and C_{max} represent the minimum and maximum value of the measurement range, while ΔC_{res} represents the measurement resolution.

	Value [pF]
$C_{\min}$	450
$C_{\max}$	600
ΔC_{res}	1

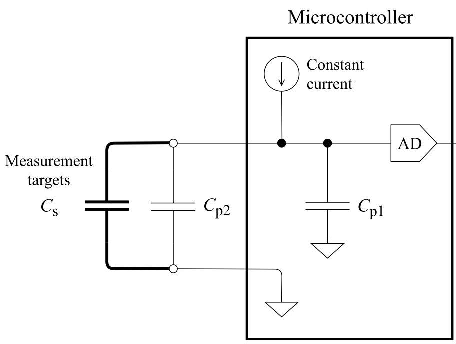

FIGURE 5. The experimental setup for the evaluation of the capacitance measurement module. C_{p1}, C_{p2} and C_S represent the internal parasitic capacitance of the microcontroller, capacitor to simulate the parasitic capacitances of the electrode array, and the measurement target for the evaluation, respectively.

TABLE 2. Selected parameters for the capacitance measurement module.

Parameter design	I [μA]	t [μs]
Applying conditional expression	5.190	433
Not applying conditional expression	2.104	200

To verify the effectiveness of satisfying conditional expressions (3), (4) and (8) in selecting the parameters, two patterns of measurements were carried out, one with and another without the conditional expressions applied when selecting the parameters of the capacitance measurement module. The parameters of the capacitance measurement module selected in each case are shown in Table 2. In all cases, values V_{ref} and b were set as 5 V and 10 bits, respectively.

The measurement results are shown in Fig. 6 and Table 3. The measured values of the LCR meter, used as a comparator, and the capacitance measurement module are the horizontal and vertical axes, respectively.

When the conditional expression (3), (4) and (8) was applied to the parameters, it showed $RMSE = 0.39$ pF for 7 measurement point which could be regarded as an allowable error since the resolution was set as 1 pF.

On the other hand, the measurement result without applying the conditional expression was $RMSE = 2.57$ pF, which appeared to be larger than that of the desired resolution 1 pF.

From this result, it was confirmed that the capacitance measurement module satisfying the desired performance can be designed by applying conditional expressions.

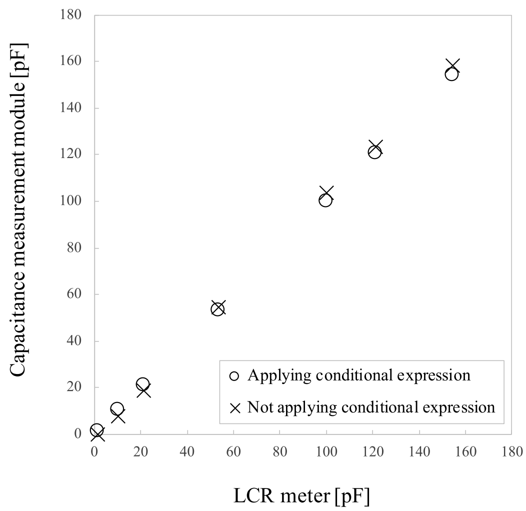

FIGURE 6. Measurement result of the capacitance measurement module. The capacitance measurement module with and without applying conditional expression are compared with the measured values of the LCR meter (true value).

TABLE 3. Measurement error of the capacitance measurement module, with and without applying conditional expression. Here, the true values are the measurement results of the LCR meter.

True value [pF]	Measurement Error [pF]	
	Applying conditional expression	Not applying conditional expression
1.33	0.15	-1.33
10.35	0.19	-2.50
21.17	-0.14	-2.44
53.54	-0.59	1.02
100.10	-0.25	3.50
121.45	-0.74	1.97
154.23	-0.08	3.89

B. POSTURE MEASUREMENT USING CAPACITANCE MEASUREMENT MODULE WITH ELECTRODE ARRAY

The posture of the subject on the electrodes was measured by using the electrode array and the capacitance measurement module. In order to simulate a sleeping environment for the measurement, we used a cloth (cotton, 0.2 mm thick) that simulates a bed sheet and covered the electrode array. One adult male subject was measured wearing nightwear (material: cotton, thickness: 0.4 mm top and 0.6 mm bottom). The subject was instructed to lie on the electrode array in two different postures: supine and left lateral. The parameters of the capacitance measurement module were set to same values in Table 1, which were $I = 5.190$ μA and $t = 433$ μs, respectively.

As mentioned above, the posture is detected by measuring the capacitance of all the electrodes and obtaining the silhouette of the subject from their distribution. For this reason, it is necessary to precisely measure the difference in capacitance between the human body and the electrodes with high accuracy. However, as shown in Fig. 7, each individual electrode of the electrode array has a different

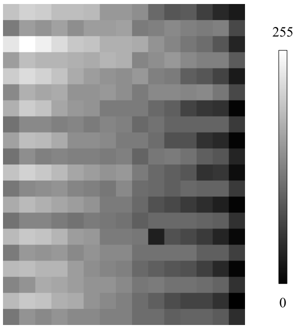

FIGURE 7. Distribution of parasitic capacitance across the electrode array.

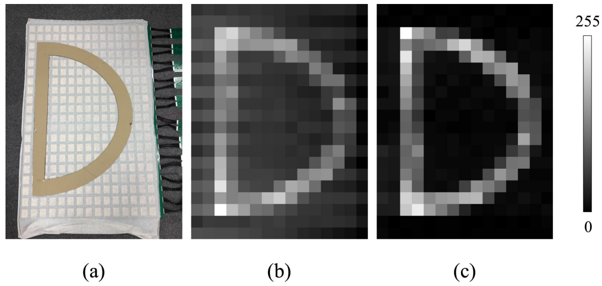

FIGURE 8. Capacitance distribution of the character-shaped metallic object. (a) Measurement environment. (b) Raw data of the capacitance distribution. (c) After background subtraction process of capacitance distribution.

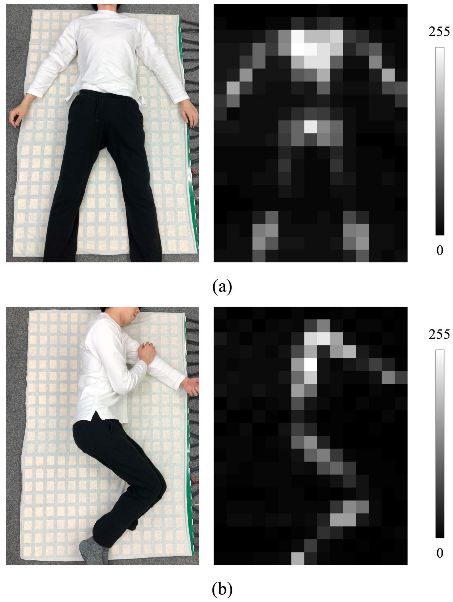

FIGURE 9. Capacitance distribution of the human posture. (a) Subject in supine posture. (b) Subject in left lateral posture.

parasitic capacitance, due to the effect of the wiring length and other electrical factors. Therefore, background subtraction was utilized to remove the effect of parasitic capacitance and extract only the changes in capacitance caused by the subject. Specifically, two measurements were made before and after the subject lying on the electrode array, and only the capacitance values that changed depending on the subject's presence were measured by subtracting the data of these two measurements.

First, the effect of the background subtraction was verified using a character-shaped metallic object with a conductive bottom surface, as shown in Fig. 8. Here, Fig. 8 (c) is the result of differential scanning of the raw data in Fig. 8 (b) with the background data in Fig. 7. As shown in Fig. 8 (b), the silhouette of the object is obscured in the data before the background subtraction because of the parasitic capacitance. On the other hand, as shown in Fig. 8 (c), the parasitic capacitance is canceled out in the data after the background subtraction, and the capacitance is detected only at the electrode where the object is located, and the shape of the object is clearly captured.

Next, we measured the posture of a human subject using the method described above, and the results are shown in Fig. 9. As shown in Fig. 9, the measurement results of the capacitance distribution accurately captured the outlines of the subject, according to the subject's posture on the electrode array. When scoping into the distribution of capacitance for each region of the human body, the electrodes around the waist and knee in Fig. 9 (a), and the electrodes around the waist and shin in Fig. 9 (b) show smaller capacitance than other electrodes. This is due to the fact that the capacitance appears to be inversely proportional to the distance between the human body and the electrodes, and the fact that the unevenness of the human skeleton creates a distance between the human body and the ground surface at certain locations. These results indicate that the configuration of the electrode array and the capacitance measurement module can be used to measure the posture.

C. ELECTROCARDIOGRAM MEASUREMENT USING ECG MEASUREMENT MODULE

The electrode array and the ECG measurement module were used to measure the electrocardiogram of several subjects. Five healthy male subjects #A-#E (22-25 years old, 1.57-1.84 m height, 45-73 kg) were instructed to lie on the electrode array in three postures. The experiments in this study were conducted with the approval of the Hosei University Research Ethics Committee.

First, the subject's postural information on the electrode array was measured by the method described in the previous section. Next, the experimenter selected three electrodes (+, −, GND) to be used for the measurement according to the postural information and the capacitance between the human body. The multiplexer was used to switch the connection of these three electrodes to the ECG measurement module, and the electrocardiogram was measured with a sampling frequency of 800 Hz and a resolution of 14 bits. In addition, in order to evaluate the reliability of the electrocardiogram, the true value was synchronously recorded by a reference system (NeXus-10 MKII) with a sampling frequency of 512 Hz and a resolution of 24 bits. The electrodes for the reference system was fixed to the II induction arrangement regardless of the subject's posture.

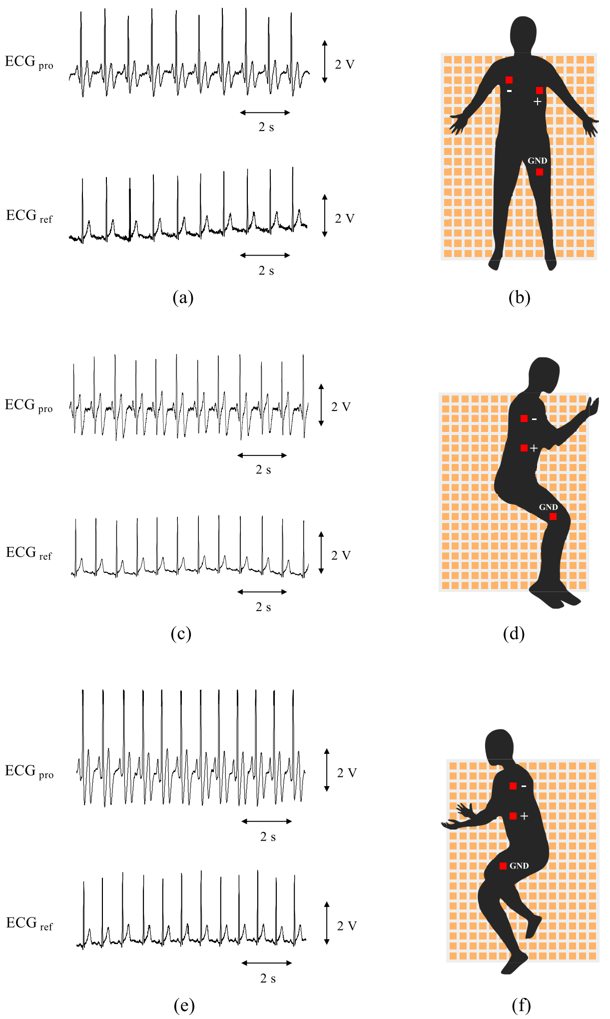

FIGURE 10. Electrocardiogram synchronously measured by the ECG measurement module and the reference system of one typical subject #E in three postures. The subscripts "ref" and "pro" refer to the reference system and the proposed ECG measurement module. (a) Synchronized electrocardiogram in supine posture and (b) electrodes used for the ECG measurement module. (c) Synchronized electrocardiogram in left lateral posture and (d) electrodes used for the ECG measurement module. (e) Synchronized electrocardiogram in right lateral posture and (f) electrodes used for the ECG measurement module.

The electrocardiogram measured by the ECG measurement module and the reference system of one typical subject #E in three postures are shown in Fig. 10. All electrocardiogram signals measured by the ECG measurement module were synchronized with the reference system. The signals were recorded when the subject remained stationary where the signal was stable and less affected by body movement. Fig. 10 (b), (d), and (f) show the electrodes (+, −, GND) actually used for the measurement in each posture.

Fig. 10 (a), (c), and (e) show that the QRS complex along with the P-wave and T-wave, which are characteristic waveforms of the electrocardiogram, are clearly visible. However, they also show that the shape of the electrocardiogram signals depend on the posture to some extent, and it appears that the

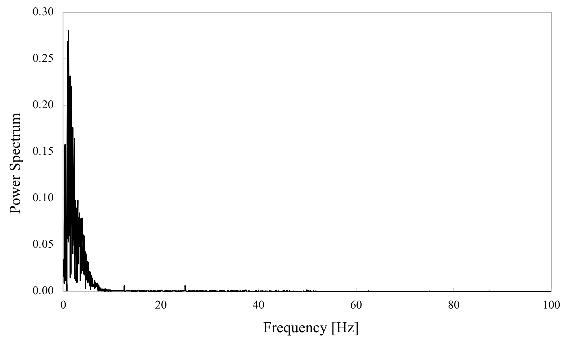

FIGURE 11. Frequency analysis of the electrocardiogram of subject #E in the supine posture measured by the ECG measurement module. The results show a fundamental frequency (approximately 1 Hz) corresponding to the electrocardiogram signal cycle and its harmonic components.

TABLE 4. Correlation coefficient r and mean absolute percentage error (Error [%]) of the RR intervals between the proposed ECG measurement module and reference system. The correlation coefficient and error rate were derived in three postures for subjects #A-#E.

Subject	Supine		Left lateral		Right lateral	
	r	Error [%]	r	Error [%]	r	Error [%]
#A	1.00	0.20	0.94	0.29	0.98	0.34
#B	0.99	0.28	0.99	0.19	0.97	0.39
#C	0.99	0.34	0.99	0.30	0.97	1.57
#D	0.98	0.34	1.00	0.04	1.00	0.22
#E	1.00	0.09	0.97	0.55	1.00	0.07

signals mostly matches with the reference system in the case of the supine posture.

The frequency analysis of the electrocardiogram, measured by the ECG measurement module of one typical subject #E in supine posture, is shown in Fig. 11. The results show the fundamental frequency (approximately 1 Hz) corresponding to the electrocardiogram signal cycle (usually expressed in RR intervals) and its harmonic components, which is a reasonable result [22].

Table 4 shows the correlation coefficient r and mean absolute percentage error (MAPE) of the RR intervals measured from subjects #A-#E in three postures. The error rate [%] was defined by the equation:

$$M = \frac{1}{n}\sum_{t=1}^{n}\left|\frac{A_t - F_t}{A_t}\right| \times 100 \quad [\%] \tag{9}$$

where A_t is the reference value and F_t is the measured value.

The RR intervals of all subjects #A-#E measured by the ECG measurement module show high correlation, regardless of the posture, which is at the same level with the study [23].

Table 5 shows the accuracy of the R-wave measured by the ECG measurement module in the supine posture. Accuracy has been calculated with reference to the study [24]. Here, when the peak of the R-wave measured by the

TABLE 5. Accuracy [%] of the R-wave measured by the proposed ECG measurement module in the supine posture.

Subject	Accuracy [%]
#A	92.31
#B	90.91
#C	91.67
#D	88.89
#E	100.00
MN	92.76
SD	3.01

TABLE 6. Measurement conditions of Fig. 12 (a)-(d). The table describes the appropriateness of the selected electrodes in terms of electrode arrangement and contact state.

	Electrode arrangement	Contact state
(a)	Good	Good
(b)	Good	Bad
(c)	Bad	Good
(d)	Bad	Bad

ECG measurement module appears within ±3 ms of that measured by reference system, they were considered to be correctly identified. Then, the accuracy [%] was defined by the equation:

$$ACC = \frac{TP + TN}{TP + TN + FP + FN} \times 100 \quad [\%] \tag{10}$$

where TP represents the number of R-waves correctly identified, FP is the number of R-waves incorrectly identified (i.e. the time difference exceeds 3 ms), FN is the number of R-waves appearing only in the reference system, and TN is the number of R-waves appearing only in the ECG measurement module.

The results show that the mean value of the accuracy for subjects appeared to be 92.76%, which is equivalent to 93.2% of the study [24].

These results indicate that the ECG measurement module has equivalent performance compared with other studies [23], [24], though it should be noted that measurement in the supine posture is preferably suitable to obtain electrocardiogram with wave patterns closer to the reference system.

Finally, some experiments were conducted to clarify the necessity of selecting the appropriate electrodes considering body posture and capacitance between the human body, which is the basic premise of the proposed sensor. The experimental results and measurement conditions are shown in Fig. 12 and Table 6, respectively.

The experiment was conducted by one male subject #E, lying in the supine posture. All electrocardiograms were recorded synchronously by the ECG measurement module and the reference system. The measurement conditions were as shown in Table 6. Since the electrocardiogram was measured in the supine posture, electrode arrangement

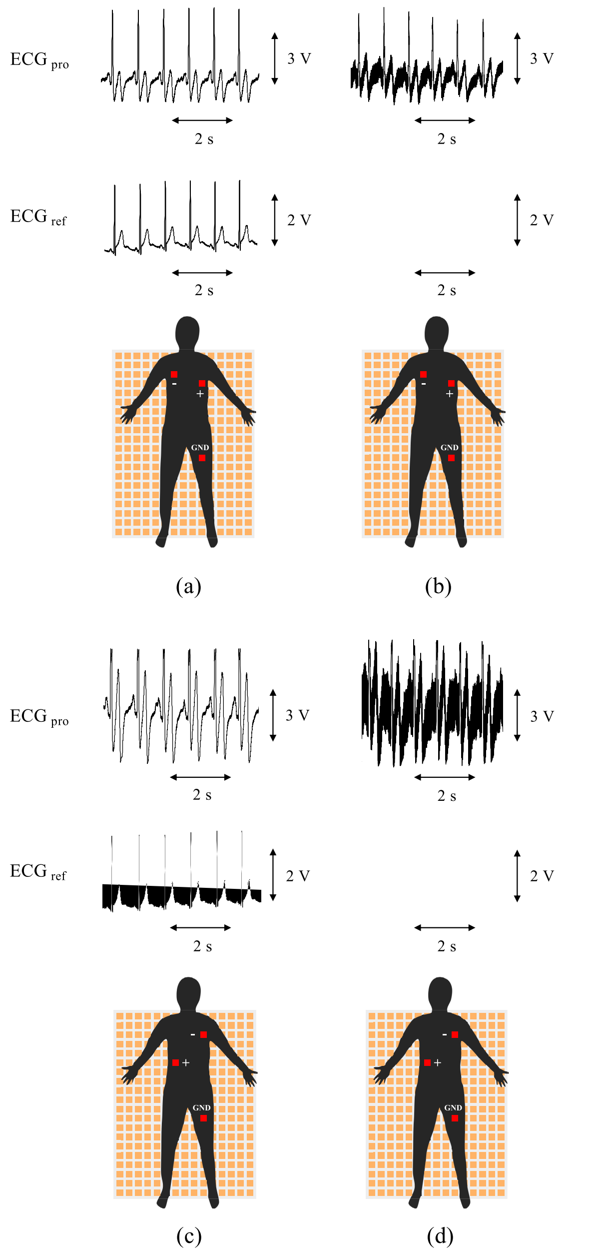

FIGURE 12. Synchronous electrocardiogram measurement results of subject #E in the supine posture in different measurement conditions. The subscripts "ref" and "pro" refer to the reference system and the proposed ECG measurement module. The illustration at the bottom show the electrodes used for the measurement of the ECG measurement module. The measurement conditions are (a) Good electrode arrangement and contact state (b) Good electrode arrangement and bad contact state (c) Bad electrode arrangement and good contact state (d) Bad electrode arrangement and contact state, as summarized in Table 6.

corresponding to the II induction was assumed as "good", and the electrode arrangement perpendicular to that of the II induction was assumed as "bad". Also, the capacitance between the human body (i.e. contact state) was assumed as "good" when there was a short distance between the electrode and body, and was assumed as "bad" when they were not. The illustration at the bottom of Fig. 12 describes the electrodes actually used for the measurement of the ECG measurement module.

Fig. 12 (a) shows that measurements with good electrode arrangement and contact state result in clear signals. Next, when the contact state is bad, as shown in Fig. 12 (b) and (d), the electrocardiogram signal becomes noisy, making it difficult to detect the QRS complex along with the P-wave and T-wave. The results of Fig. 12 (c) and (d) show that the peaks of the T-waves of the electrocardiogram signals become unusually large compared to that shown in Fig. 12 (a), which suggest that the signal distorts when the electrode arrangement is inappropriate. From these results, it can be said that it is important to select the appropriate electrodes considering both body posture and capacitance between the human body.

V. CONCLUSION AND FUTURE WORK

The authors have been working on the realization of a novel unconstrained electrocardiogram measurement system using arrayed electrodes that is robust with respect to the physical body differences and postural variations, and therefore, has a potential to replace the Holter electrocardiograph for use during sleep.

In this study, as the core of the system, we designed and developed a new sensor that can measure both body posture and electrocardiogram with common arrayed electrodes and verified its effectiveness through evaluation experiments.

From the experimental results, it was confirmed that the posture of the subject on the electrode array could be obtained from the capacitance distribution data by using the capacitance measurement module adjusted with the appropriate design parameters. Also, the QRS complex along with the P-wave and T-wave, which are characteristic waveforms of the electrocardiogram, were clearly observed especially in case of supine posture by using the ECG measurement module. Furthermore, RR intervals measured by the ECG measurement module in supine posture showed high correlation and accuracy with the reference system, and reached the performance of recent studies [23], [24]. Therefore, these results indicate the potential usefulness of the designed and developed sensor.

In the future, based on the sensor developed in this study, we plan to complete the electrocardiogram system by automating the process of selecting electrodes considering body posture and capacitance between the human body.

REFERENCES

[1] S. Tsugane, "Why has Japan become the world's most long-lived country: Insights from a food and nutrition perspective," *Eur. J. Clin. Nutrition*, pp. 1–8, Jul. 2020.

[2] Y. G. Lim, K. K. Kim, and S. Park, "ECG measurement on a chair without conductive contact," *IEEE Trans. Biomed. Eng.*, vol. 53, no. 5, pp. 956–959, May 2006.

[3] T. Matsuda and M. Makikawa, "ECG monitoring of a car driver using capacitively-coupled electrodes," in *Proc. 30th Annu. Int. Conf. IEEE Eng. Med. Biol. Soc.*, Aug. 2008, pp. 1315–1318.

[4] T. Maruyama, M. Makikawa, N. Shiozawa, and Y. Fujiwara, "ECG measurement using capacitive coupling electrodes for man-machine emotional communication," in *Proc. IEEE/ICME Int. Conf. Complex Med. Eng.*, May 2007, p. 378.

[5] A. Ueno, Y. Shiogai, and Y. Ishiyama, "A primary study of indirect ECG monitor embedded in a bed for home health care," *IEEJ Trans. Electron., Inf. Syst.*, vol. 127, no. 10, p. 1792–1799, 2007.

[6] Y. Nishida, M. Takeda, T. Mori, H. Mizoguchi, and T. Sato, "Monitoring patient respiration and posture using human symbiosis system," in *Proc. IEEE/RSJ Int. Conf. Intell. Robot Syst. Innov. Robot. Real-World Appl. (IROS)*, 1997, pp. 632–639.

[7] H. M. Van der Loos, N. Ullrich, and H. Kobayashi, "Development of sensate and robotic bed technologies for vital signs monitoring and sleep quality improvement," *Auton. Robots*, vol. 15, pp. 67–79, Jul. 2003.

[8] Y.-W. Liu, Y.-L. Hsu, and W.-Y. Chang, "Development of a bed-centered telehealth system based on a motion-sensing mattress," *J. Clin. Gerontol. Geriatrics*, vol. 6, no. 1, pp. 1–8, Mar. 2015.

[9] M. Laurino, L. Arcarisi, N. Carbonaro, A. Gemignani, D. Menicucci, and A. Tognetti, "A smart bed for non-obtrusive sleep analysis in real world context," *IEEE Access*, vol. 8, pp. 45664–45673, 2020.

[10] K. Sakai, G. Nakagami, N. Matsui, H. Sanada, A. Kitagawa, E. Tadaka, and J. Sugama, "Validation and determination of the sensing area of the KINOTEX sensor as part of development of a new mattress with an interface pressure-sensing system," *Biosci. trends*, vol. 2, no. 1, pp. 36–43, 2008.

[11] J. M. Kortelainen and J. Virkkala, "FFT averaging of multichannel BCG signals from bed mattress sensor to improve estimation of heart beat interval," in *Proc. 29th Annu. Int. Conf. IEEE Eng. Med. Biol. Soc.*, Aug. 2007, pp. 6685–6688.

[12] S. Guo, Y. Kato, H. Ito, and T. Mukai, "Development of rubber-based flexible sensor sheet for care-related apparatus," *SEI Tech. Rev.*, vol. 75, pp. 125–131, Oct. 2012.

[13] T. Mukai, K. Matsuo, Y. Kato, A. Shimizu, and S. Guo, "Determination of locations on a tactile sensor suitable for respiration and heartbeat measurement of a person on a bed," in *Proc. 36th Annu. Int. Conf. IEEE Eng. Med. Biol. Soc.*, Aug. 2014, pp. 66–69.

[14] H. Wong, J. Kaufman, B. Baylis, J. M. Conly, D. B. Hogan, H. T. Stelfox, D. A. Southern, W. A. Ghali, and C. H. Ho, "Efficacy of a pressure-sensing mattress cover system for reducing interface pressure: Study protocol for a randomized controlled trial," *Trials*, vol. 16, no. 1, p. 434, Dec. 2015.

[15] W. Y. Chang, C. C. Huang, C. C. Chen, C. C. Chang, and C. L. Yang, "Design of a novel flexible capacitive sensing mattress for monitoring sleeping respiratory," *Sensors*, vol. 14, no. 11, pp. 22021–22038, 2014.

[16] W. Y. Chang, C. C. Huang, C. C. Chen, C. C. Chang, and C. L. Yang, "An enhanced sensing application based on a flexible projected capacitive-sensing mattress," *Sensors*, vol. 14, no. 4, pp. 6922–6937, 2014.

[17] M. Erkinjuntti, K. Vaahtoranta, J. Alihanka, and P. Kero, "Use of the SCSB method for monitoring of respiration, body movements and ballistocardiogram in infants," *Early Hum. Develop.*, vol. 9, no. 2, pp. 119–126, Feb. 1984.

[18] B. Eilebrecht, A. Schommartz, M. Walter, T. Wartzek, M. Czaplik, and S. Leonhardt, "A capacitive ECG array with visual patient feedback," in *Proc. Annu. Int. Conf. IEEE Eng. Med. Biol.*, Aug. 2010, pp. 6539–6542.

[19] E. M. Kardoulaki, K. N. Glaros, A. G. Katsiamis, and E. M. Drakakis, "An 8Hz, 0.1 μW, 110+ dBs sinh CMOS bessel filter for ECG signals," in *Proc. Int. Conf. Microelectron. (ICM)*, Dec. 2009, pp. 14–17.

[20] B. B. Winter and J. G. Webster, "Driven-right-leg circuit design," *IEEE Trans. Biomed. Eng.*, vol. BME-30, no. 1, pp. 62–66, Jan. 1983.

[21] K. K. Kim, Y. K. Lim, and K. S. Park, "Common mode noise cancellation for electrically non-contact ECG measurement system on a chair," in *Proc. IEEE Eng. Med. Biol. 27th Annu. Conf.*, Jan. 2006, pp. 5881–5883.

[22] M. C. Abay, J. W. Ibanez, and M. J. Segismundo, "FFT analysis of ECG signals in EDF format," Cultural Assoc. Manila Univ., Manila, Philippines, Tech. Rep., Oct. 2010.

[23] M. Takano and A. Ueno, "Noncontact in-bed measurements of physiological and behavioral signals using an integrated fabric-sheet sensing scheme," *IEEE J. Biomed. Health Informat.*, vol. 23, no. 2, pp. 618–630, Mar. 2019.

[24] M. Takano, S. Yamagishi, T. Ohmuta, Y. Fukuoka, and A. Ueno, "Non-contact simultaneous measurements of electrocardiogram and respiratory movements using capacitive sheet electrodes," *Adv. Biomed. Eng.*, vol. 6, pp. 28–36, 2017.

SOUSUKE NAKAMURA (Member, IEEE) received the B.E., M.E., and Dr.Eng. degrees from The University of Tokyo, Tokyo, Japan, in 2005, 2007, and 2012, respectively, all in electrical engineering. In 2012, he joined Chuo University, as an Assistant Professor. In 2016, he was with Hosei University, as a Lecturer. Since 2018, he has been with Hosei University, as an Associate Professor. His current research interests include human augmentation, health monitoring, and robotics and wireless power transfer. He is also a member of the Society of Instrument and Control Engineers of Japan, the Japan Society for Fuzzy Theory, the Institute of Electrical Engineers of Japan, the Virtual Reality Society of Japan, and the Robotics Society of Japan.

NAOKI KAMIYAMA (Member, IEEE) received the B.E. degree in electrical and electronic engineering from Hosei University, Japan, in 2019, where he is currently pursuing the M.E. degree. His research interests include biomedical measurement, electrocardiography, biomedical electrodes, health information management, and artificial neural networks.

YUTO ARIMA received the B.E. and M.E. degrees from Hosei University, Japan, in 2018 and 2020, respectively, both in electrical and electronic engineering. He is currently an Electrical Engineer in developing healthcare devices. His research interests include biomedical measurement, electrocardiography, biomedical electrodes, and health information management.

TETSUO NAKAMURA (Member, IEEE) received the B.E. degree in electrical engineering from Keio University, Japan, in 1980. He received the Ph.D. degree from Hosei University, Japan, in 2012. From 1980 to 1991, he was involved in the research and development of radio frequency systems, analog LSI, and communication systems at Pioneer Corporation. From 1993 to 2014, he developed and created business plans for sensor LSI and bio measurement LSI at JEPICO Corporation, as the Engineering Director. Since 2017, he has been with Meisei University, as a Project Professor. He has published articles on the design of analog LSIs and holds 130 patents in analog LSI technology, filter technology, radio frequency systems, and bio measurement systems.